İSTANBUL TECHNICAL UNIVERSITY ★ INSTITUTE OF SCIENCE AND TECHNOLOGY

IMAGING OF PERFECTLY MAGNETIC CONDUCTING ROUGH SURFACE THROUGH SINGLE FREQUENCY SINGLE VIEW DATA

M.Sc. Thesis by
Çağdaş GENÇ, B.Sc.

Department : Elecgtronics and Telecommunication Engineering
Programme: Teelcommunication Engineering

Supervisor : Prof. Dr. Ibrahim AKDUMAN

FABRUARY 2008

ACKNOWLEDGEMENT

I would like to express my immense gratitude to Prof. Dr. İbrahim AKDUMAN who gave me the opportunity to do research under his supervision for his precious guidance and supports during this study. I would also like to deeply thank to Assoc. Prof. Dr. Ali YAPAR for his great help and many valuable contributions to this thesis.

December-2007 Çağdaş GENÇ

TABLE OF CONTENTS

	Page No:
LIST OF ABBREVIATIONS	iii
LIST OF FIGURES	iv
LIST OF SYMBOLS	v
SUMMARY	vi
ÖZET	vii
1 INTRODUCTION	1
2 SCATTERING OF ELECTROMAGNETIC BY PERFECT MAGNETIC ROUGH SURFACE	3
3 SOLUTION OF THE INVERSE PROBLEM	7
3.1 Reconstruction of scattering field from the measured data	7
3.2 An iteratively reconstruction of the surface	7
4 NUMERICAL IMPLEMENTATION	11
5 CONCLUSIONS	17
REFERENCES	18

LIST OF ABBREVIATIONS

LIST OF FIGURES

Page No:

2.1 Geometry of the problem. 4

2.2 The complex ν-plane. 5

4.1 Exact and reconstructed values of the surface for noise-free data. 12

4.2 Exact and reconstructed values of the surface for incident angle $\phi_0 = \frac{\pi}{6}$ 13

4.3 Exact and reconstructed values of the surface for a sinusoidal surface having 2 times greater amplitude than the one in (Fig 4.1). . 14

4.4 Exact and reconstructed values of the surface for a sinusoidal surface having 3 times larger number of fluctuations than the one in (Fig 4.1). 14

4.5 Exact and reconstructed values of the surface (4.1) for different level of noise. 15

4.6 Exact and Reconstructed values of a corrugated surface. 15

4.7 Exact and Reconstructed variations of a random surface. 15

4.8 Exact and Reconstructed variations of a random surface. 16

4.9 Exact and Reconstructed variations of a random surface. 16

LIST OF SYMBOLS

$\vec{E}$	:	Electric field vector
μ_0	:	Permeability of the free space
ε_1	:	Dielectric permittivity of the upper half space
ε_2	:	Dielectric permittivity of the lower half space
σ	:	Conductivity of the half space
k	:	Wavenumber of the half space
ω	:	Angular frequency
λ	:	Wavelength
ϕ_0	:	Incidence angle
u_i	:	Incident field
u_0	:	Total field in absence of rough surface
u_s	:	Scattered field from the rough surface
$\tilde{u}$	:	Total field
σ_r	:	Rms height
ℓ_c	:	Correlation length
σ_{2D}	:	Scattering width
Γ	:	Interface of two half spaces
δ	:	Dirac delta distribution

IMAGING OF PERFECTLY MAGNETIC CONDUCTING ROUGH SURFACE THROUGH SINGLE FREQUENCY SINGLE VIEW DATA

SUMMARY

In this thesis, a novel and effective algorithm is derived for the solution of inverse scattering problems related to perfectly magnetic conducting rough surface. Such problems are of great importance in electromagnetic theory due to the their potential applications in practice such as modeling of ground wave propagation, microwave remote sensing, optical system measurements, underwater acoustics, non-destructive testing etc.

The surface is illuminated by a time-harmonic plane wave from the half space above the surface and the scattered field is assumed to be measured on a certain line. The method is obtained for a single illumination at a fixed frequency. In order to give a suitable representation of the electromagnetic field in the half-space above the surface, the half space is separated into two parts by an estimated plane. Then the electric field vector above the this plane is represented as spectrum of plane waves while Taylor series expansion is used in the region between the surface and estimated plane. Though the special representation of the field mentioned above, the measured scattered data leads to obtain the total electric field in the whole half space. The perfect magnetic conductivity of the surface requires that the normal derivative of the total electric field vanishes, and application of this condition yields a non-linear equation whose unknown is the surface function. The non-linear equation is solved iteratively via the Newton method and reconstruction in the least square sense.

MÜKEMMEL MANYETİK İLETKEN YÜZEYLERİN TEK FREKANSTA TEK ÖLÇÜM VERİSİYLE GÖRÜNTÜLENMESİ

ÖZET

Bu tez çalışmasında, engebeli ve mülemmel manyetik iletken özelliklerine sahip bir yüzeyden ters saçılma probleminin çözümü için yeni ve etkin bir yöntem verilmiştir. Söz konusu problemler, yer dalgası yayılımının modellenmesi, mikrodalga uzaktan algılama teknikleri, sualt akustik çalışmaları gibi pek çok uygulama alanına sahip olmaları sebebiyle elektromagnetik teoride büyük öneme sahiptirler.

Problem çözümünde düzlemsel bir kaynak tarafından aydınlatılan ve yüzeyden saçılan dalgalar, belirli bir uzaklıkta ölçülmler kullanılmaktadır. Bu metod kullanılarak, tek öçümle, tek frekansta alınana verilerle yüzey yeniden oluşturulmuştur. Takip edilen yöntem sırasında, yüzeyim üzerinde kalan yarım uzay, bir tahmini yüzey ile iki parçaya ayrılmıştır. Ölçümler sonucu elde edilen verilerden yararlanılarak elektrik alan bu tahmini yüzeyde hesaplanmış ve bu yüzeyden bulunmaya çalşılan gerçek yüzey doğrultusunda elektrik alan taylor serisine açılmıştr. Son olarak mülemmel manyetik iletken özelliklere sahip yüzey üzerinde normal türevlerin tanımlanması ile lineer olmayan problem iterasyon yöntemi ile çözülmüştür.

1 INTRODUCTION

Imaging of an inaccessible rough surface constitutes an important class of problems in inverse scattering theory due to the large domain of applications such as microwave remote sensing, optical system measurements, underwater acoustics, non-destructive testing etc. In these kinds of problems one tries to recover the location and shape, as well as the surface characteristics of an unknown surface through scattered field measurements in a certain domain. The surface to reconstructed can be perfect electric of magnetic conductor, or it may be an interface separating two half-spaces. Although several exact and numerical methods have been developed for the solution of these problems they can be improved to obtain more effective and faster algorithms. As far as we know, most of the inversion schemes in the open literature are concerned with the reconstruction of surfaces with small perturbations[1-5]. A large number of studies were done under the Kirchhoff approximation where the rough surface is assumed to be locally planar [4-6]. A simple FFT-based approach for surfaces having small variations is given in [3] where the problem is reduced to the solution of two integral equations that can be solved approximately. An approximate inversion scheme under the Rytov approximation is addressed in [7]. In [8] the problem is reduced to the solution of a pair of coupled integral equations with two unknown functions in the case of grazing-incidence. As far as can be observed, among the above-mentioned methods the one given in [3] has the highest surface profile limits.

Most of the above methods are derived for perfectly electric conducting surface. On the other hand, as far as we know not much work have been done for the perfect magnetic conducting (PMC) surface although they have applications in practical such as modeling of ground wave propagation, microwave remote sensing, optical system measurements, underwater acoustics, non-destructive testing etc.

The main aim of this thesis is to give a new, simple and fast method to determine the location and shape of a perfectly magnetic conducting rough surface. For the sake of simplicity, we consider surfaces having a variation in one direction. The surface is reconstructed using the illumination by a single plane monochromatic wave and the near field measurements of the scattered field are performed on a line parallel to the mean surface. The novelty of the method is that the lossy half-space above the surface is first separated into two parts by an estimated plane, and then the scattered field in the upper region above this plane is expressed in terms of a Fourier transform while it is expanded into a Taylor series in the lower part. The boundary condition on the PMC surface requires that the normal derivative of the total electric field should vanish. The use of this condition allows the reduction of the problem to the solution of a non-linear equation for the unknown surface function. Note that the resulting non-linear equation contains both the surface function and its derivative as unknowns. The non-linear equation is solved iteratively via the classical Newton method, i.e.: the problem is linearized in the Newton sense and the realty linear system is solved by an iterative schema. In this iteration procedure the required derivatives of the unknown surface function are calculated numerically. Since the solution is sensitive to errors in the data, a regularization in the least square sense is applied. The method yields satisfactory reconstructions for slightly rough surface profiles. The resolutions of the reconstructions obtained here are slightly higher than those given in [3]. A time factor $\exp(-i\omega t)$ is assumed and omitted.

The organization of the thesis is as follows: In Section 2 a new method for the scattering of electromagnetic waves from a locally rough surface is given. An Iterative Reconstruction method is given in Section 3. Numerical results are given in Section 4 and a conclusion is presented in Section 5. A time factor $e^{-i\omega t}$ is assumed and omitted throughout the thesis.

2 SCATTERING OF ELECTROMAGNETIC BY PERFECT MAGNETIC ROUGH SURFACE

In this section, a general theory for the scattering of electromagnetic waves from PMC rough surface is given, and a special representation for the electromagnetic field in the half-space above the surface is derived, which is suitable for the inverse scattering problem that will be taken into account in section 3.

Consider the two-dimensional scattering problem illustrated in figure 1. In this configuration Γ_0 is a perfectly magnetic conducting smooth surface which is defined by the relation $x_2 = f(x_1)$ where $f(x_1)$ is a single-valued function and has continuous first-order derivatives for all x_1 [9, p:2]. Γ_0 is assumed to be locally rough, i.e.: $f(x_1)$ differs from zero over a finite interval. The half-space above the surface Γ_0 is filled with a non-magnetic simple material whose dielectric permittivity and conductivity are ε and σ, respectively. The inverse scattering problem considered here consists in recovering the location and the shape of the surface Γ_0, i.e.: $f(x_1)$ from a set of scattered field measurements performed on the line $x_2 = \ell$. To this aim, the surface Γ_0 is illuminated by a time-harmonic plane wave whose electric field vector $\vec{E}^i$ is always parallel to the Ox_3 axis, namely;

$$\vec{E}^i = (0, 0, u^i(x_1, x_2)) \tag{2.1}$$

with

$$u^i(x_1, x_2) = e^{-ik(x_1 \cos\phi_o + x_2 \sin\phi_o)} \tag{2.2}$$

where ϕ_0 is the incidence angle while k is the square root of $k^2 = \omega^2\varepsilon\mu_0 + i\omega\sigma\mu_0$. Due to the homogeneity in the x_3 direction, the total and scattered electric field vectors will have only x_3 components and the problem is reduced to scalar one.

Let $u(x)$ denote the total electric field in the half-space

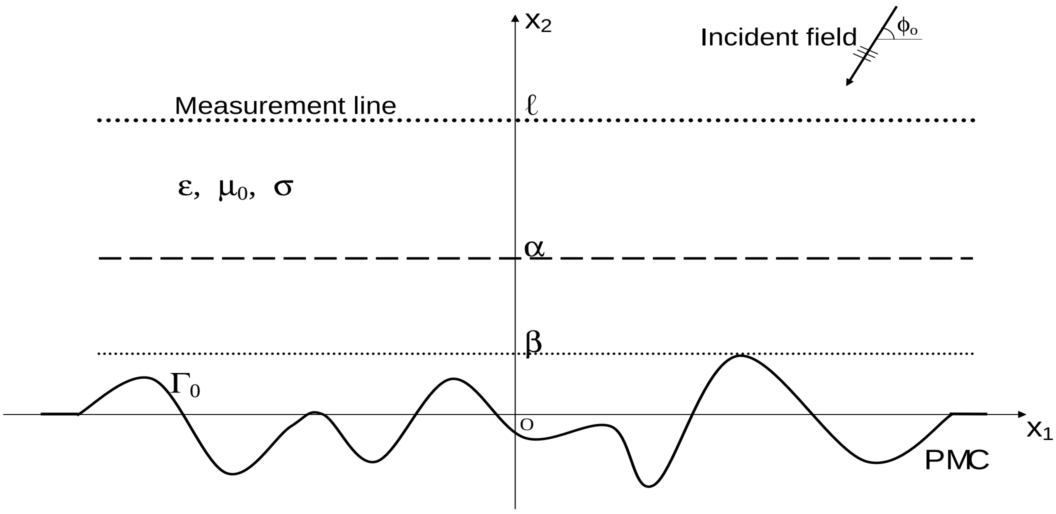

Figure 2.1: Geometry of the problem.

$x_2 > f(x_1)$ where $x = (x_1, x_2)$ is the position vector in R^2.

$u(x)$, satisfies the reduced wave equation

$$\Delta u + k^2 u = 0 \tag{2.3}$$

under the boundary condition

$$\frac{\partial u(x)}{\partial n} = 0 \quad , \quad x \in \Gamma_0 \tag{2.4}$$

when Γ is the normal vector of the surface directed to the upper half-space. Then the scattered field, $u^s(x)$, is the difference

$$u^s(x) = u(x) - u^i(x) - u^r(x) \quad , \quad x_2 > f(x_1) \tag{2.5}$$

and satisfies the reduced wave equation

$$\Delta u^s + k^2 u^s = 0 \ , \quad x_2 > f(x_1) \tag{2.6}$$

with the boundary condition

$$\frac{\partial u^s(x)}{\partial n} = -\frac{\partial u^i(x)}{\partial n} - \frac{\partial u^r(x)}{\partial n} \quad , \quad x \in \Gamma_0 \tag{2.7}$$

and the radiation condition for $|x| \to \infty$. In (2.3), $u^r(x)$ denotes the reflected field from the perfectly magnetic conducting plane $x_2 = 0$ and given by

$$u^r(x) = e^{-ik(x_1 \cos\phi_o - x_2 \sin\phi_o)}. \tag{2.8}$$

Consider now the Fourier transform of $u^s(x)$ with respect to x_1 , namely,

$$\hat{u}^s(\nu, x_2) = \int_{-\infty}^{+\infty} u^s(x) e^{-i\nu x_1} dx_1. \tag{2.9}$$

Note that (2.7) is valid only in the region $x_2 > \beta$ with $\beta = \max f(x_1)$, $\forall x_1 \in (-\infty, \infty)$ (see figure 2.1), where there is no physical discontinuity in the x_1-direction. Then the Fourier transform of (4) yields

$$\frac{d^2 \hat{u}^s}{dx_2^2} - \gamma^2(\nu)\hat{u}^s = 0 \quad , \quad \nu \in L \quad , \quad x_2 > \beta \tag{2.10}$$

where

$$\gamma(\nu) = \sqrt{\nu^2 - k^2}. \tag{2.11}$$

Here L stands for a horizontal straight line in the regularity strip of $\hat{u}^s$ in the complex ν-plane (see Fig. 2.2). The asymptotic behavior of $u(x)$ as $x_1 \to \pm\infty$ has a symmetry and consequently, the regularity strip also includes the real ν-axis. Thus without loss of generality, L can be considered as real ν-axis [10]. The square root function in (2.9) is defined in the complex ν-plane cut as shown in Fig. 2.2 such that $\gamma = -ik$ as $\nu \to 0$ [11, p:459].

A solution to (2.8) can be obtained very easily and one gets

$$\hat{u}^s(\nu, x_2) = A(\nu) e^{-\gamma x_2} \quad , \quad x_2 > \beta \tag{2.12}$$

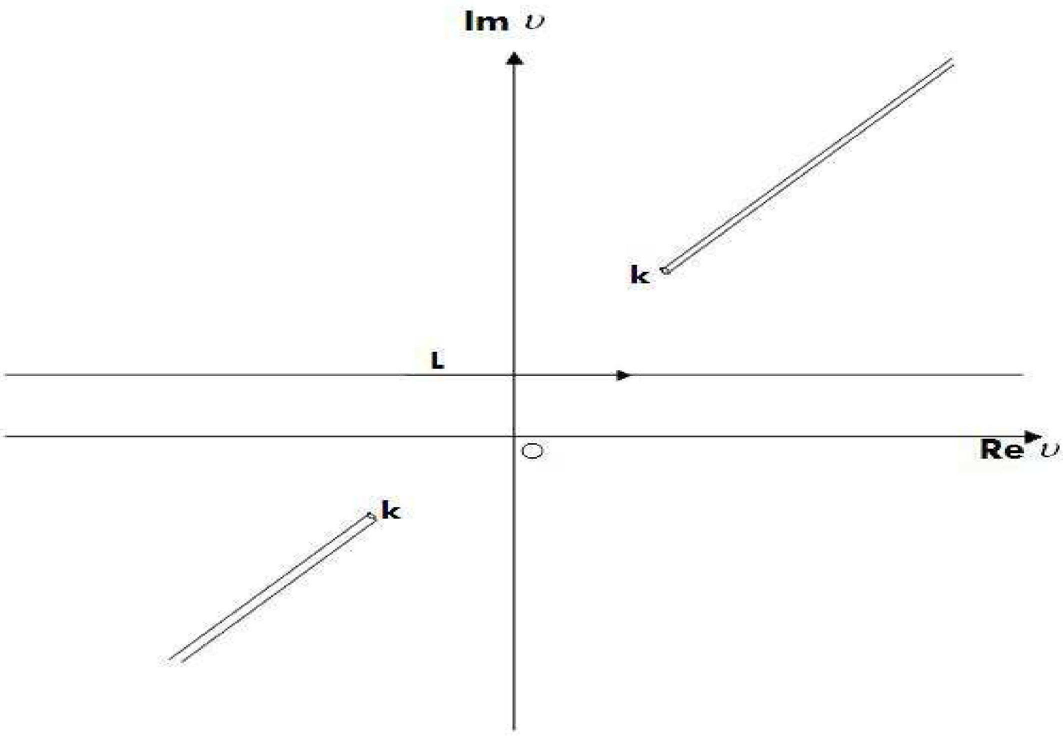

Figure 2.2: The complex ν-plane.

with the radiation condition taken into account. Here A is a coefficient to be determined. The scattered field in the region $x_2 > \beta$ can then be obtained through the inverse Fourier transform integral

$$u^s(x) = \frac{1}{2\pi} \int_L A(\nu) e^{-\gamma x_2} e^{i\nu x_1} d\nu \quad , \; x_2 > \beta \tag{2.13}$$

Note that $u^s(x)$ given by (2.11) satisfies the radiation condition as $|x| \to \infty$. This can be shown by evaluating the integral on the right hand side of (2.11) asymptotically for $|x| \to \infty$ through classical saddle point technique [11].

The scattered field below $x_2 = \beta$ can be obtained by using the field $u^s(x)$ given by (2.11). To this aim, $u^s(x)$ is expanded into a Taylor series in terms of x_2 around the plane $x_2 = \alpha$, where $\beta < \alpha < \ell$, as follows [9, p:110]:

$$u^s(x) = \sum_{m=0}^{\infty} \frac{1}{m!} \frac{\partial^m u^s(x_1, \alpha)}{\partial x_2^m} (x_2 - \alpha)^m, \quad x_2 \in [f(x_1), \alpha) \tag{2.14}$$

The m'th order derivatives of $u^s(x)$ at $x_2 = \alpha$ appearing in the right hand side of (2.12) can be obtained very easily from (2.11) and one has

$$\frac{\partial^m u^s(x_1,\alpha)}{\partial x_2^m} = \frac{1}{2\pi}\int_L (-1)^m \gamma^m A(\nu) e^{-\gamma\alpha} e^{i\nu x_1} d\nu. \tag{2.15}$$

Since $u^s(x)$ is a regular function of x_2 the series (2.12) is always convergent down to the surface Γ_0 [9]. Thus to write the solution of (2.4), the half-space over the surface Γ_0 is first separated into two regions $x_2 > \alpha$ and $x_2 \in [f(x_1), \alpha)$, and the scattered field in both regions are expressed through (2.13) and (2.14), respectively.

The pair (2.13) and (2.14) can be used to solve either direct or inverse scattering problems related to the configuration in Fig.1. In the direct problem the surface, consequently the function $f(x_1)$, is known and one tries to obtain the spectral coefficient $A(\nu)$ via the boundary condition in (2.7.). In the inverse problem the function $f(x_1)$ has to be determined from the measured values of the scattered field $u^s(x)$ on the line $x_2 = \ell$, namely, $u^s(x_1, \ell)$. In the following an iterative method to reconstruct $f(x_1)$ from these measured data is given.

3 SOLUTION OF THE INVERSE PROBLEM

3.1 Reconstruction of scattering field from the measured data

Let us assume that $u^s(x_1, \ell)$ is known for all $x_1 \in (-\infty, \infty)$. Then by putting $x_2 = \ell$ in (11) one gets

$$u^s(x_1, \ell) = \frac{1}{2\pi} \int_L A(\nu) e^{-\gamma \ell} e^{i\nu x_1} d\nu. \tag{3.1}$$

Hence the spectral coefficient $A(\nu)$ can be determined from (14). Indeed (14) is the inverse Fourier transform of the function $A(\nu)e^{-\gamma\ell}$ and one has

$$A(\nu) = \hat{u}^s(\nu, \ell) e^{\gamma\ell} \tag{3.2}$$

where $\hat{u}^s(\nu, \ell)$ denotes the Fourier transform of $u^s(x_1, \ell)$ with respect to x_1, namely,

$$\hat{u}^s(\nu, \ell) = \int_{-\infty}^{+\infty} u^s(x_1, \ell) e^{-i\nu x_1} dx_1. \tag{3.3}$$

Since $A(\nu)$ is known, the scattered field in the half-space $x_2 > f(x_1)$ can be obtained through (11) and (12). In the practical applications $u^s(x_1, \ell)$ is only known at a finite number of points on the line $x_2 = \ell$ through the measurements. In such a case the integral appearing on the right hand side of (16) is evaluated by using one of the known quadrature techniques which gives approximate values of the spectral coefficient $A(\nu)$ from (15).

3.2 An iteratively reconstruction of the surface

The reconstruction of the surface Γ_0 can now be achieved by searching the points where the boundary condition (2.4) is satisfied. Note that since the surface is not known, one cannot directly calculate the normal derivative appearing in (2.4). On the other hand, we have the expressions

$$\frac{\partial}{\partial s} = \frac{1}{\sqrt{1+[f']^2}}(\frac{\partial}{\partial x_1} + f'\frac{\partial}{\partial x_2}) \tag{3.4}$$

and

$$\frac{\partial}{\partial n} = \frac{1}{\sqrt{1+[f']^2}}(-f'\frac{\partial}{\partial x_1} + \frac{\partial}{\partial x_2}) \tag{3.5}$$

for the tangential and normal derivatives on Γ where f' denotes the derivation of f with respect to x_1. Thus the inverse scattering problem is reduced to finding the points when the condition

$$\frac{1}{\sqrt{1+[f']^2}}(-f'\frac{\partial u}{\partial x_1} + \frac{\partial u}{\partial x_2}) = 0 \tag{3.6}$$

is satisfied.

To this aim, $x_2 = f(x_1)$ is first put in (3.6) and the infinite series in (3.14) is approximated by truncating the summation at an appropriate number M. The resulting expression can be written in a compact form as follows:

$$F_M(f) = 0 \tag{3.7}$$

where F_M is the non-linear operator given by

$$F_M(f) = \frac{\partial}{\partial n}[\sum_{m=0}^{M} \frac{1}{m!}\frac{\partial^m u^s(x_1,\alpha)}{\partial x_2^m}(f(x_1)-\alpha)^m + e^{-ik(x_1\cos\phi_o + f(x_1)\sin\phi_o)} - e^{-ik(x_1\cos\phi_o - f(x_1)\sin\phi_o)}] \tag{3.8}$$

$$F_M(f) = \frac{1}{\sqrt{1+[f']^2}}(-f'\frac{\partial}{\partial x_1} + \frac{\partial}{\partial x_2})[\sum_{m=0}^{M} \frac{1}{m!}\frac{\partial^m u^s(x_1,\alpha)}{\partial x_2^m}(f(x_1)-\alpha)^m + e^{-ik(x_1\cos\phi_o + f(x_1)\sin\phi_o)} - e^{-ik(x_1\cos\phi_o - f(x_1)\sin\phi_o)}] \tag{3.9}$$

Note that for given data $u^s(x_1, \ell)$ the coefficients $\frac{\partial^m u^s(x_1,\alpha)}{\partial x_2^m}$ in (3.25) are all known through the relations (3.2) and (2.15). Thus the reconstruction problem is reduced to the solution of non-linear equation (3.7) for the unknown function f.

The convergence rate of the Taylor series in (2.14) for $x_2 = f(x_1)$ is related to $|f(x_1) - \alpha|$ which is the distance between the surface Γ_0 and the plane $x_2 = \alpha$ for a certain x_1. If the plane $x_2 = \alpha$ close to the surface and the surface function $f(x_1)$ is a slightly varying one, the distance $|f(x_1) - \alpha|$ becomes small and the series in (2.14) can be approximated by choosing a small truncation number M. To select the appropriate M, a threshold value δ is chosen and the series is truncated at the smallest M, satisfying

$$\left| \frac{1}{M!} \frac{\partial^M u^s(x_1, \alpha)}{\partial x_2^M} (\min[f(x_1)] - \alpha)^M \right| < \delta. \tag{3.10}$$

The non-linear equation (3.7) can be solved iteratively via Newton method [12]. To this aim, for an initial guess f_0, the nonlinear equation (3.7) is replaced by the linearized equation

$$F_M(f_0) + F_M'(f_0)\Delta f = 0 \tag{3.11}$$

where $\Delta f = f - f_0$, that needs to be solved for Δf in order to improve an approximate boundary Γ_0 given by the function f_0 into a new approximation with surface function $f_0 + \Delta f$. In (3.12) F_M' denotes the Frechet derivative of the operator F with respect to f [13]. It can be shown that F_M' reduces the ordinary derivative of F_M with respect to f.

The Newton method consists in iterating this procedure, i.e.: in solving

$$F_M'(f_i)\Delta f_{i+1} = -F_M(f_i), \quad i = 0, 1, 2, 3, ... \tag{3.12}$$

for Δf_{i+1} to obtain a sequence of approximations through $f_{i+1} = f_i + \Delta f_{i+1}$.

It is obvious that this solution will be sensitive to errors in the derivative of F_M in the vicinity of zeros. To obtain a more stable solution, the unknown Δf

is expressed in terms of some basis functions $\phi_n(x_1)$, $n = 1, \ldots, N$, as a linear combination

$$\Delta f(x_1) = \sum_{n=1}^{N} a_n \phi_n(x_1). \tag{3.13}$$

A possible choice of basis functions consists of trigonometric polynomials [12]. Then (3.12) is satisfied in the least squares sense, that is, the coefficients $a_1, \ldots, a_N$ in (3.13) are determined such that for a set of grid points $x_1^1, \ldots, x_1^J$ the sum of squares

$$\sum_{j=1}^{J} \left| F'_M(f(x_1^j)) \sum_{n=1}^{N} a_n \phi_n(x_1^j) + F_M(f(x_1^j)) \right|^2 \tag{3.14}$$

is minimized. The number of basis functions N in (3.13) can be considered as a kind of regularization parameter. Choosing N too large leads to instabilities due to the ill-posedness of the underlying inverse problem. Choosing N too small results in poor approximation quality. Hence one has to compromise between stability and accuracy and in this sense N serves as a regularization parameter.

Notice that the propagation of the scattered wave from $x_2 = \ell$ to $x_2 = \alpha$ is also ill-posed. This can be seen by substituting $A(\nu)$ given by (3.2) into (2.13) and considering a real wave-number k. In such a case the integral appearing in (2.13) will have the term $e^{\gamma(\ell-\alpha)}\hat{u}^s(\nu, \ell)$ which represents the propagation of the measured data from $x_2 = \ell$ to $x_2 = \alpha$. Then by taking

$$\gamma(\nu) = \begin{cases} \sqrt{\nu^2 - k^2}, & |\nu| > k \\ -i\sqrt{k^2 - \nu^2}, & |\nu| < k \end{cases} \quad , \; for \;\; \nu, k \in R \tag{3.15}$$

into account [11] one can easily conclude that the errors in the data, i.e.: errors in $\hat{u}^s(\nu, \ell)$, will be amplified by the factor $e^{\gamma(\ell-\alpha)}$ for $|\nu| > k$. This causes the problem to be ill-posed. Therefore some regularization is required. This can be done by restricting the integral on L appearing in (2.13) to a finite interval. Accuracy of the approximation requires this interval to be large and stability requires it to be small. In the following this interval was chosen as $(-k, k)$, corresponding to the non-evanescent components of the scattered wave.

4 NUMERICAL IMPLEMENTATION

In this section some numerical results which demonstrate the validity of the method, as well as the effects of some parameters on the reconstructions will be given.

The half-space over the surface is assumed to be free space. In all cases the operating frequency is 300 MHz and the height of the measurement line is $\ell = 5\lambda$ where λ is the free-space wavelength. The scattered data which should be collected by real measurements are calculated synthetically by solving the associated direct problem through the single layer potential approach [14] for locally rough surfaces with a length of locality L_0. The integral appearing in (2.13) is evaluated numerically by using the trapezoidal rule. In all examples random noise is added to the simulated data of the scattered field. In particular a random term $n_\ell |u_m^s| e^{2ir_d\pi}$ is added to each scattering field values u_m^s, n_ℓ being the noise level and r_d a random number between 0 and 1. In the application of least squares solution the basis functions are chosen as $\phi_n(x_1) = e^{i2\pi n x_1/L_0}$, $n = 0, \pm 1, \ldots, \pm N$, and the number N is determined by trial and error.

The first example is devoted to the validation of the proposed method. To this end we consider a sinusoidal slightly rough surface given by

$$f(x) = 0.1\lambda cos(\frac{2\pi}{12\lambda}x) \tag{4.1}$$

The surface is illuminated from normal direction. The number of terms in the Taylor series M=27 and number of basis function in the Least Square regularization N=120 The exact and reconstructed surface obtained after 6 iteration and illustrated in Figure 4.1. Obviously, reconstructed surface is completely the same with the exact one. This example show that for surface having a small variation the method yields quite accurate reconstruction.

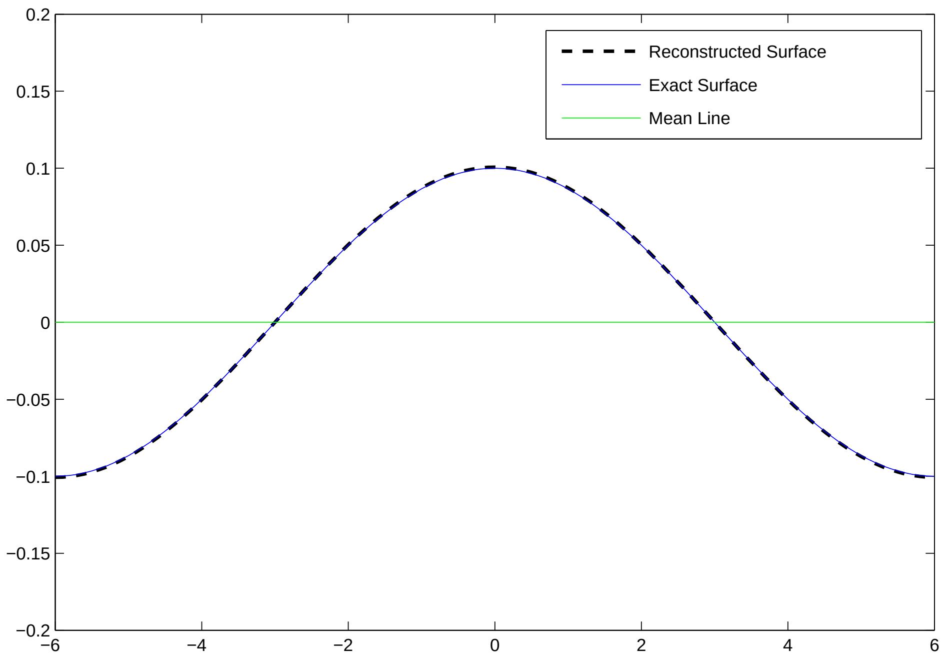

Figure 4.1: Exact and reconstructed values of the surface for noise-free data.

In order to see the effect of the incident direction, the surface (4.1) is illuminated by a plane wave of an incident direction $\phi_0 = \frac{\pi}{6}$ and the exact and reconstructed values of the surface are presented in Figure 4.2. For this illumination, as can be observed, the reconstructions in the right part of the surface are not as accurate as the left part. This is due to the fact that the right end part of the surface stays in the shadow region and the measured data does not contain enough information about this part of the surface. For that reason, one can conclude that best reconstruction can be obtained for the normal incidence case.

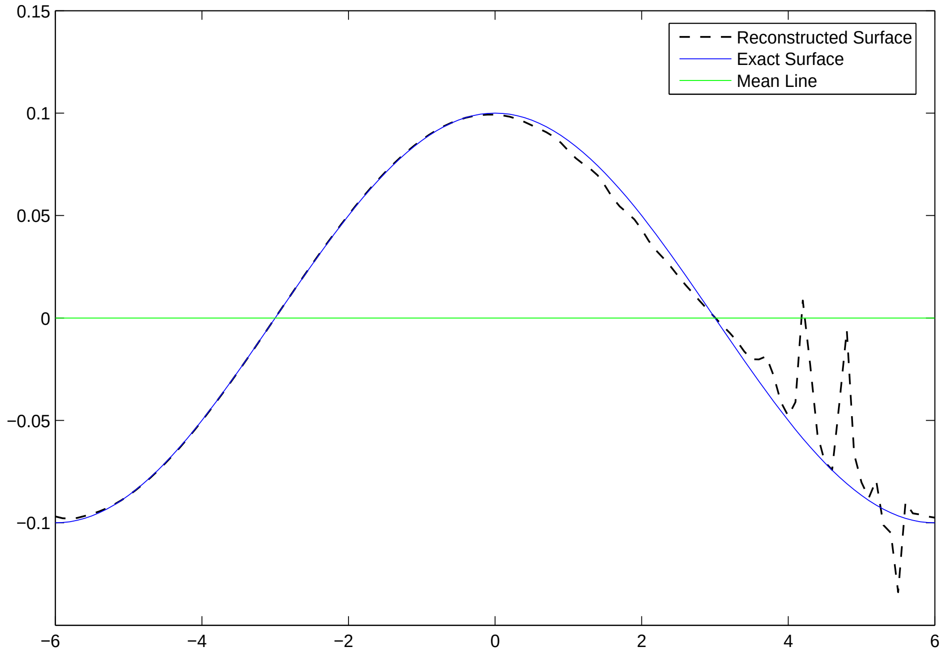

Figure 4.2: Exact and reconstructed values of the surface for incident angle $\phi_0 = \frac{\pi}{6}$.

In figure 4.3, the exact and reconstructed values of the sinusoidal surface which is 2 times greater then the one in Fig. 4.1. All the parameter are the same for the example in Fig 4.1. As can be seen, the accuracy of the method fails for surface having large variations. In other words, the proposed method yields accurate reconstruction slightly varying surfaces.

For a sinusoidal surface having large number of fluctuations, we present the results in Figure 4.4. The parameters are kept the same as in the previous example.

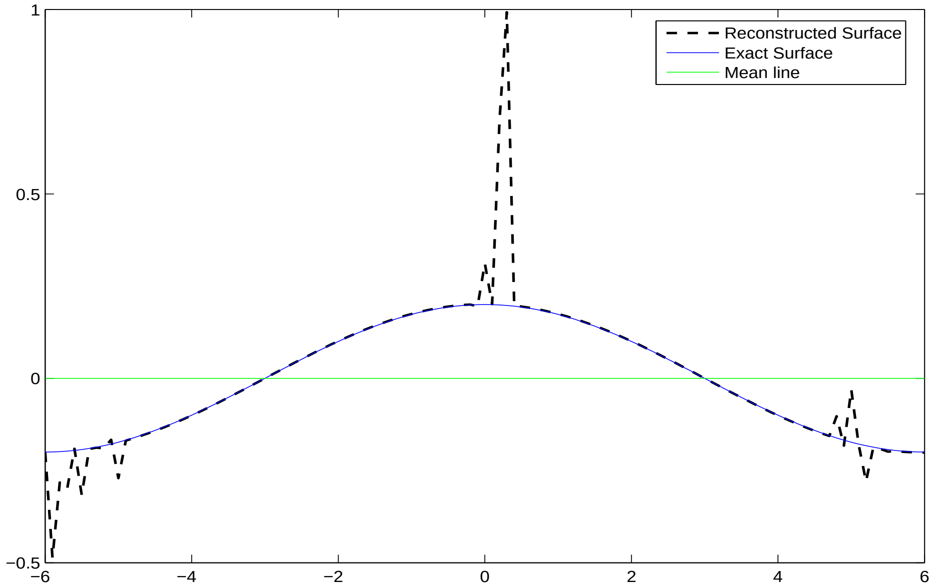

Figure 4.3: Exact and reconstructed values of the surface for a sinusoidal surface having 2 times greater amplitude than the one in (Fig 4.1).

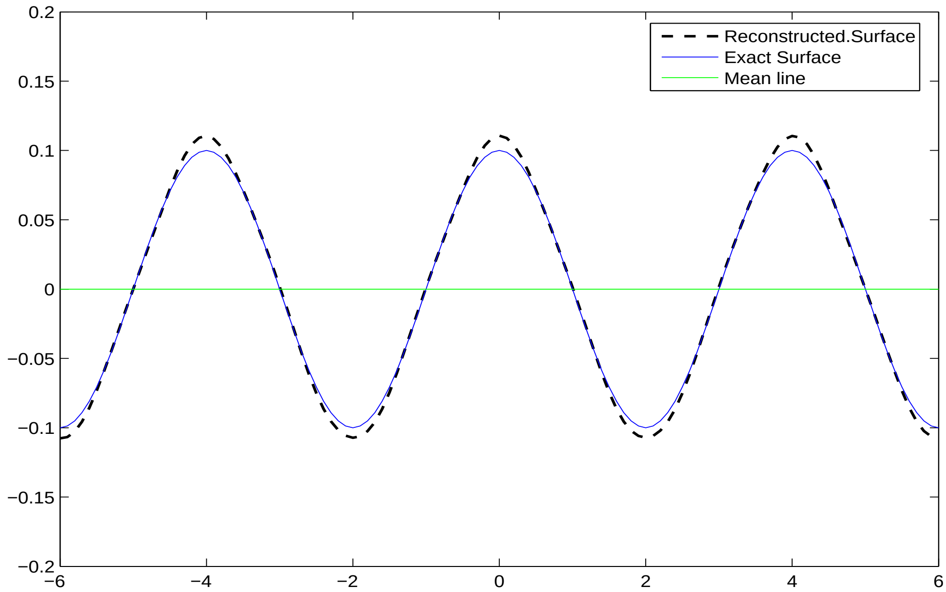

Figure 4.4: Exact and reconstructed values of the surface for a sinusoidal surface having 3 times larger number of fluctuations than the one in (Fig 4.1).

To see the effect of the noise level is the reconstructions, we added %5 and %10random noise to the measured data for the surface given in Fig 4.1. By keeping all the parameters same with obtained the reconstruction given in Figure 4.5.

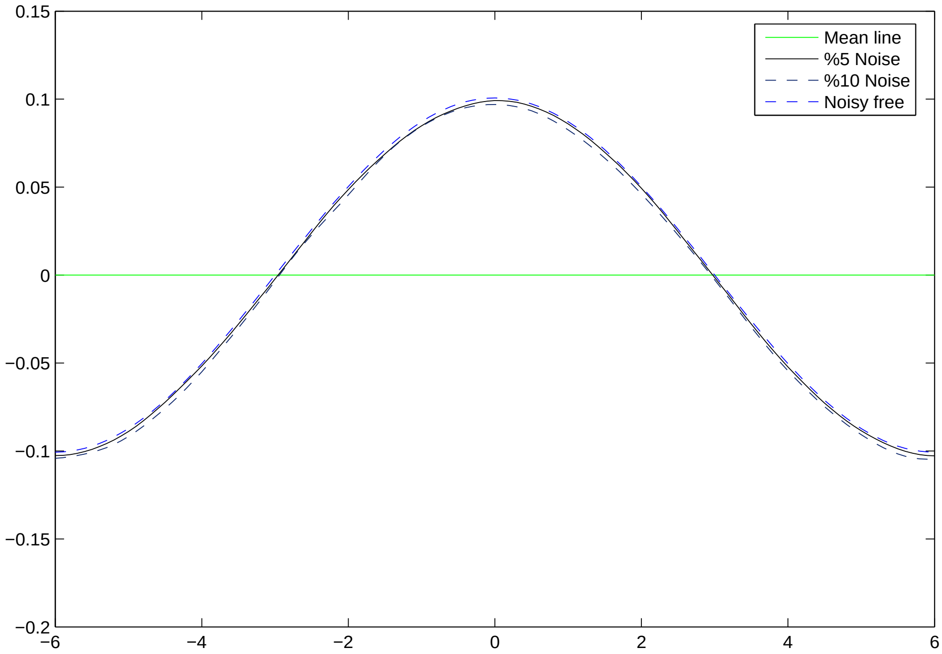

Figure 4.5: Exact and reconstructed values of the surface (4.1) for different level of noise.

In the figure (4.6), (4.7), (4.8) and (4.9) exact and reconstructed values of the surfaces having different veriations are demonstrated. For the surfaces in (4.6), (4.7), (4.8) and (4.9) have same with example in Fig 4.1.

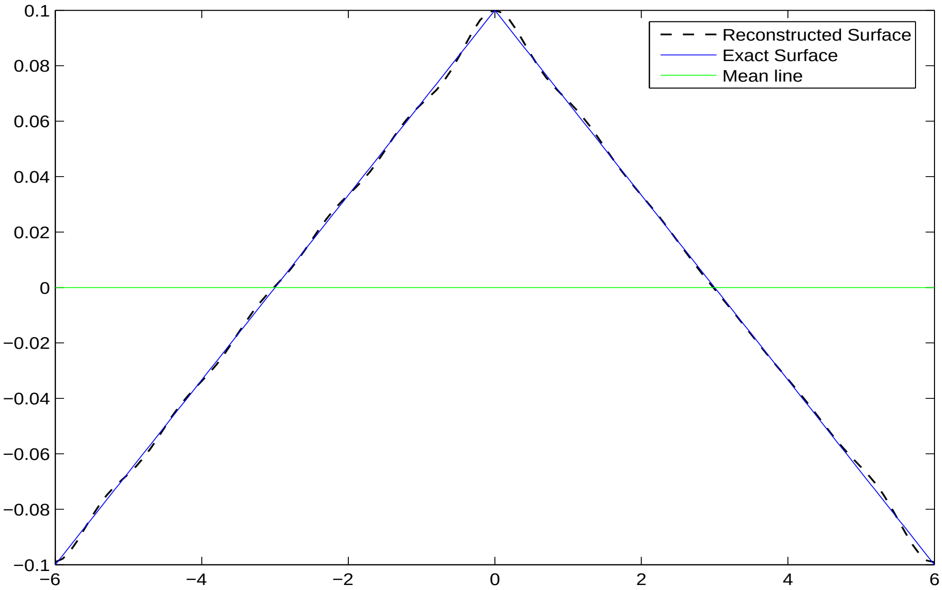

Figure 4.6: Exact and Reconstructed values of a corrugated surface.

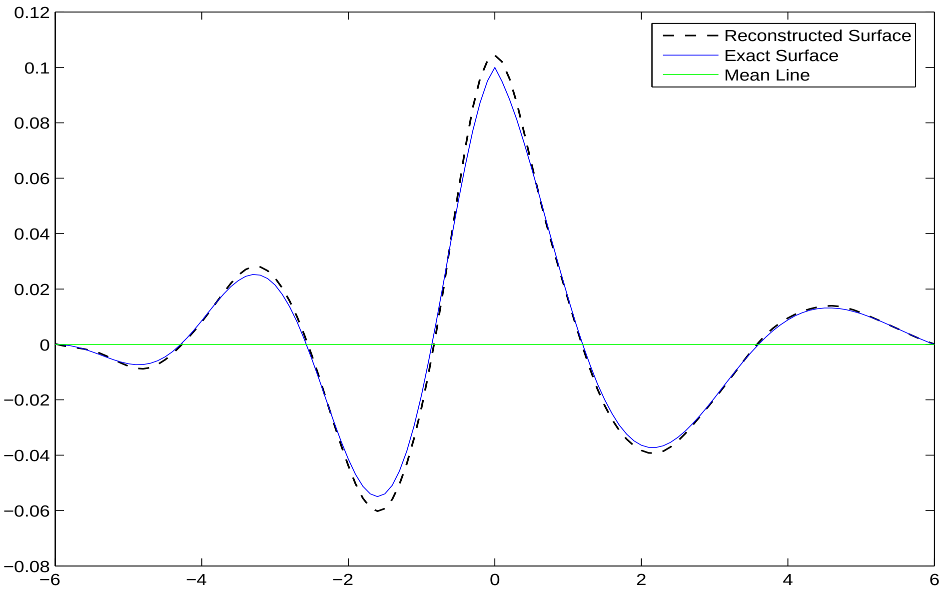

Figure 4.7: Exact and Reconstructed variations of a random surface.

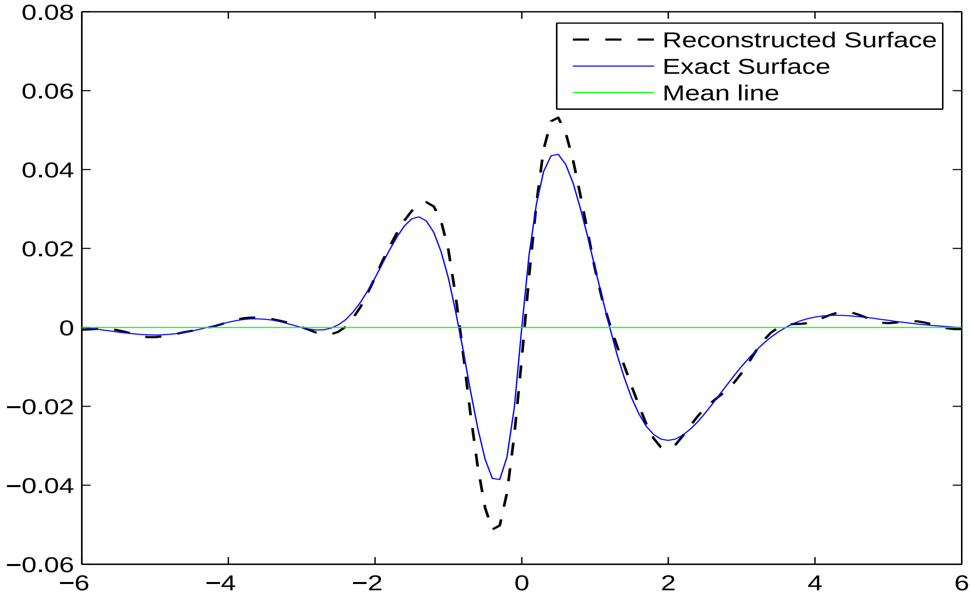

Figure 4.8: Exact and Reconstructed variations of a random surface.

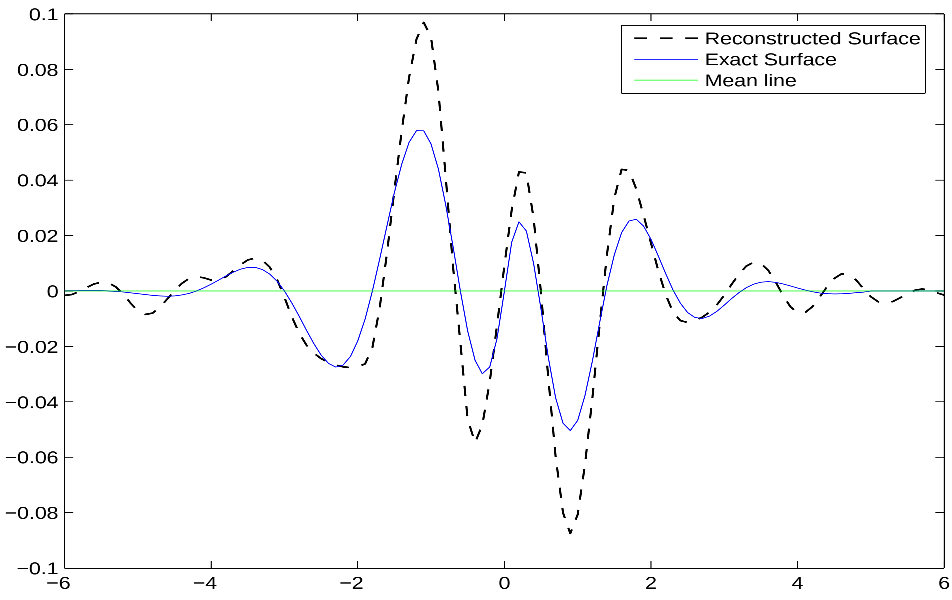

Figure 4.9: Exact and Reconstructed variations of a random surface.

5 CONCLUSIONS

An inverse scattering problem whose aim is to recover the one-dimensional profile of a perfectly magnetic conducting rough surface has been presented. Through a special representation of the scattered field in terms of Fourier transform and Taylor series the total field in the half-space over the surface is computed from measured data. The problem is then reduced to the solution of a non-linear equation which can be treated iteratively via Newton method.

This method yields satisfactory reconstructions for the surfaces having a peak-to-peak variation less than $\lambda/2$. This level of roughness is at least 5 times greater than those of the methods based on the perturbation approach and Kirchhoff approximation and comparable to that of the method given in [3] in the case of noisy data. The resolutions of the reconstructions are closely related to the number of terms in the Taylor expansion, the number of basis functions in the least squares solution and the integration limits in the numerical evaluation of the inverse Fourier transform. Furthermore, as has been shown, more terms in the Taylor series result in higher resolution. Future studies are aimed to extend the method for the rough interfaces between two dielectric half-spaces.

References

[1] Rice, SO., 1951, "Reflection of electromagnetic wave by slightly rough surfaces.", *Commun. Pure Appl. Math.*, 4, 351-378.

[2] Sanchezgil, JA. Maradudin, AA. and Mendez, ER., 1995, "Limits of validity of 3 perturbation theories of the specular scattering of light from one-dimensional, randomly rough, dielectric surfaces." *Journal of the Optical Society of America A-Optics Image Science and Vision*, 12, (7) 1547-1558.

[3] Soubret, A. Berginc, G. and Bourrely, C., 2001, "Backscattering enhancement of an electromagnetic wave scattered by two-dimensional rough layers." *Journal of the Optical Society of America A-Optics Image Science and Vision.*, 18, (11), 2778-2788.

[4] Fuks, IM. Voronovich, AG., 2000, "Wave diffraction by rough interfaces in an arbitrary plane-layered medium." *Waves in Random Media*, 10, (2), 253-272.

[5] Yarovoy, AG. de Jongh, RV. and Ligthart, LP., 2000, "Scattering properties of a statistically rough interface inside a multilayered medium", *Radio Science*, 35, (2), 455-462.

[6] Franceschetti, G. Iodice, A. Migliaccio, M. and Riccio, D., 1999, "Fractals and the small perturbation scattering model." *Radio Science*, 34, (5), 1043-1054.

[7] Chen, J. Lo, TKY. Leung, H. and Litva, J., 1996, "The use of fractals for modeling EM waves scattering from rough sea surface", *IEEE Transactions on Geoscience and Remote Sensing*, 34, (4), 966-972.

[8] Elfouhaily, T. Thompson, DR. Vandemark, D. and Chapron, B., 1999, "A new bistatic model for electromagnetic scattering from perfectly conducting random surfaces", *Waves in Random Media*, 9, (3), 281-294.

[9] Fitzgerald, RM. Maradudin, AA., 1994, "A reciprocal phase-perturbation theory for rough-surface scattering." *Waves in Random Media*, 4, (3), 275-296.

[10] Zhang, XD. Wu, ZS. and Wu, CK., 1997,"A phase perturbation technique for light scattering from randomly dielectric rough surfaces" *Chinese Physics Letters*, 14, (1), 32-35.

[11] Vazouras, CN. Yarovoy, AG. Moyssidis, MA. de Jong, RV. Fikioris, JG. and Ligthart, LP., 2000, "Application of perturbation techniques to the problem of low-frequency electromagnetic wave scattering from an air-ground interface", *Radio Science*, 35, (5), 1049-1064.

[12] Yarovoy, AG., 1996, "Small slope iteration technique for wave scattering from a rough interface of two media", *IEEE Transcations on Antennas and Propagation*, 44, (11), 1433-1437.

[13] Elfouhaily, T. Joelsen, M. Guignard, S. and Thompson, DR., 2003, "Analytical comparison between the surface current integral equation and the second-order small-slope approximation", *Waves in Random Media*, 13, (3), 165-176.

[14] Demir , MA. Johnson, JT., 2003, "Fourth-and higher-order small-perturbation solution for scattering from dielectric rough surfaces", *Journal of the Optical Society of America A-Optics Image Science and Vision*, 20, (12), 2330-2337.

[15] Johnson, JT., 1999, "Third-order small-perturbation method for scattering from dielectric rough surfaces", *Journal of the Optical Society of America A-Optics Image Science and Vision.*, 16, (11), 2720-2736.

[16] Warnick, KF. and Chew WC., 2001, "Numerical simulation methods for rough surface scattering", *Waves in Random Media*, 11, (1), R1-R30.

[17] R.T. Marchand and G.S. Brown, 1999," On the use of finite surfaces in the numerical prediction of rough surface scattering", *IEEE Transcations on Antennas and Propagation*, 47, (4), 600-604.

[18] Chan, CH. Tsang, L. and Li, Q., 1998, "Monte-Carlo simulations of large-scale one-dimensional random rough surfaces scattering at near-grazing incidence: Penetrable case", *IEEE Transcations on Antennas and Propagation*, 46, (1), 142-149.

[19] Chen, RM. West, JC., 1995, "Analysis of scattering from rough surfaces at large incidence angles using a periodic-surface moment method", *IEEE Transactions on Geoscience and Remote Sensing*, 33, (5), 1206-1213.

[20] Schwering, FK. Whitman, GM. and Triolo, AA., 2004, "New full-wave theory for scattering from rough metal surfaces- the correction current method: the TE-polarization case", *Waves in Random Media*, 14, (1), 23-60.

[21] Baudier, C. Dusseaux, R. Edee, KS. and Granet, G., 2004, "Scattering a plane wave by one-dimensional dielectric random rough surfaces-study with the curvilinear coordinate method", *Waves in Random Media*, 14, (1), 61-74.

[22] Chaikina, EI. Navarrete, AG. Mendez, ER. Martinez, A. and Maradudin, AA., 1998, "Coherent scattering by one-dimensional randomly rough metallic surfaces", *Applied Optics*, 37, (6), 1110-1121.

[23] Yang, TQ. Broschat, SL., 1992, "A comparison of scattering model results for 2-dimensional randomly rough surfaces", *IEEE Transcations on Antennas and Propagation*, 40, (12), 1505-1512.

[24] Millet, FW. and Warnick, KF., 2004,"Validity of rough surface backscattering models", *Waves in Random Media*, 14, (3), 327-347.

[25] S.F. Mahmoud, S.M. Ali and J. R. Wait, 1981, "Electromagnetic scattering from a buried cylindrical inhomogeneity inside a lossy earth", *Radio Science*, Vol.16, No.6, pp: 1285-1298, Nov.-Dec.

[26] D.A. Hill, 1988, "Electromagnetic scattering by buried objects of low contrast", *IEEE Trans. Geosci.and Remote Sensing*, Vol.26, No.2, pp: 195-203.

[27] G.A. Ellis and I. C. Peden, 1995, "An analysis technique for buried inhomogeneous dielectric objects in the precence of an air-earth interface", IEEE Trans. Geosci.and Remote Sensing, Vol.13, No.3, pp: 535-540.

[28] M.D. Vico, F. Frezza, L. Pajewski and G. Schettini, 2005, "Scattering by a finite set of perfectly conducting cylinders buried in a dielectric half-space:a spectral-domain solution", *IEEE Transaction On Antennas an Propagation*, Vol.53, No.2, pp: 719-727.

[29] P.G. Cottis and J.D. Kanellopoulos, 1992, "Scattering of electromagnetic waves from cylindrical inhomogeneities embedded inside a lossy medium with sinusoidal surface", *J. Electromagnetic Waves and Appl.*, Vol.6, No.4, pp: 445-458.

[30] P.G. Cottis, C.N. Vazouras, C. Kalamatianos and J.D. Kanellopoulos, 1996, "Scattering of TM waves from a cylindrical scatterer buried inside a two-layer lossy ground with sinusoidal surface", *J. Electromagnetic Waves and Appl.*, Vol.10, pp: 1005-1021.

[31] D.E. Lawrance and K. Sarabandi, 2002, "Electromagnetic scattering from a dielectric cylinder buried beneath a slightly rough surface", *IEEE Trans. on Antennas and Prop.*, Vol. 50, No. 10, pp. 1368-1376.

[32] T. Chiu and K. Sarabandi, 1999, "Electromagnetic scattering interaction between a dielectric cylinder and slightly rough surface", *IEEE Trans. on Antennas and Prop.*, Vol. 47, pp. 902-913,.

[33] J. T. Johnson, 2001, "Thermal emission from a layered medium bounded by a slighly rough interface", *IEEE Trans. Geosci.and Remote Sensing*, Vol.39, pp: 368-378.

[34] J. T. Johnson and R.J. Burkholder, 2001, "Coupled canonical grid/discrete dipole approach for computing scattering from objects above or below a rough interface", *IEEE Trans. Geosci.and Remote Sensing*, Vol.39, No.6 pp: 1214-1220.

[35] J. T. Johnson and R.J. Burkholder, 2004, "A study of scattering from an object below a rough surface", *IEEE Trans. Geosci.and Remote Sensing*, Vol.42, No. 1 pp: 59-66,.

[36] A. W. Morgenthaler and C.M. Rappaport, 2001, "Scattering from lossy dielectric objects buried beneath randomly rough ground: validiting the semi-analytical mode matching algorithm with 2-D FDFD", *IEEE Trans. Geosci.and Remote Sensing*, Vol.39, No. 11 pp: 2421-2428.

[37] J. Q. He, T. J. Yu, N. Geng and L. Carin, 2000, "Method of moment analysis of electromagnetic scattering from a general three-dimensional dielectric target embedded in a multilayered medium", *Radio Science*, Vol.32, pp: 305-313.

[38] M. El-Shenawee, 2003," Scattering From Multiple Objects Buried Beneath Two-Dimensional Random Rough Surface Using the Steepest Descent Fast Multipole Method", *IEEE Trans. on Geosience and Remote Sensing*, Vol. 51, No. 4.

[39] M. El-Shenawee and C. Rappaport, 2003, "Electromagnetic scattering interference between two shallow objects buried under 2-D random rough surfaces", *IEEE Microwave and Wireless Componets Letters*, Vol.13, No. 6 pp: 223-225.

[40] A. Madrazo and M. Nieto-Vesperinas, 1997, "Scattering of light and other electromagnetic waves from a body buried beneath a highly rough random surface ", *JOSA-A* , Vol.14 (8), pp:1859-1866.

[41] Sarabandi, K. and Chiu, T., 1997, " Electromagnetic scattering from slightly rough surfaces with inhomogeneous dielectric profiles", *IEEE Transcations on Antennas and Propagation* 45, (9), 1419-430.

[42] Yu, T. and Carin, L., 2002, " Parallel Extended-Born analysis of electromagnetic scattering from 3-Dimensional sub-rough surface targets, *IEEE AP Society International Symposium*, Vol.4, 260-263.

[43] A. Ishimaru, J.D. Rockway and Y. Kuga, 2000, "Rough surface Green's function based on the firs-order modified perturbation and smoothed diagram method", *Waves Random Media*, 10, pp: 17-31.

[44] Altuncu Y., Yapar A., Akduman I., "On the Scattering of Electromagnetic Waves by Bodies Buried in a Half-space with Locally Rough Interface", *IEEE Trans.on Geoscience and Remote Sensing*, (in press).

[45] Altuncu Y., Akduman I., Yapar A., 2005, "On the Scattering of Electromagnetic Waves by Bodies Buried in a Half-space with Locally Rough Interface", *International Conference on Electromagnetics in Advanced Applications*, Torino-Italy.

[46] Nehari, Z., 1975, *Conformal Mapping*, Dover, New York.

[47] Tsang, L., Kong, JA. and Ding, KH., 2000, *Scattering of Electromagnetic Waves*, John Wiley and Sons, USA.

[48] M. Idemen, 1973, "Maxwell's Equations in the Sense of Distributions", *IEEE Trans. Antennas and Propagat.*, Vol.21 (5), pp.736-738.

[49] Felsen, LB. and Marcuvitz, N., 1973, *Radiation and Scattering of Waves*, Printice Hall, New Jersey.

[50] Harrington, RF., 1968, *Field Computation by Moment Methods*, Macmillan, Newyork.

[51] J.A. Richmond, 1965,"Scattering by a dielectric cylinder of arbitrary cross section shape", *IEEE Trans. on Antennas and Prop*, Vol.13 (3), pp.334-341.

[52] Ishimaru, A., 1991, *Electromagnetic Wave Propagation, Radiation and Scattering*, Prentice Hall, New Jersey.

[53] Chew, WC., Jandyala, V., Lu, CC., Michielssen, E., Song, JM. and Zhao, JS., 1997, "Fast multilevel techniques for solving integral equations in electromagnetics" *Asia Pacific Microwave Conference*, p.457-460.

[54] Yapar, A., Ozdemir, O., Sahinturk, H., Akduman, I., 2006, "A Newton Method for the Reconstruction of Perfectly Conducting Slightly Rough Surface Proiles", *IEEE Trans. on Antennas and Prop*, Vol.54 (1), pp.334-341.

CODES

Direct and inverse problem simulation

Periodic Rough Surface

clear; clc; format long tic,

phi$_0 = 0; f = 3. * 10^8; omeg = 2. * pi * f; epsr1 = 1.; eps0 = (1E-9)/(36. * pi); mu0 = 4*pi*(1E-7); ak0 = omeg*sqrt(eps0*mu0); lambda_0 = 2.*pi/ak0;$

Nc=27; Nc1=Nc+1;

tolerans=10$^-$5;

P=12*lambda$_0; someparametersforthedefinitionofthesurfacefunctiony = f(x)p1 = 0.1*lambda_0; someparametersforthedefinitionofthesurfacefunctiony = f(x)p2 = 0.1*lambda_0; someparametersforthedefinitionofthesurfacefunctiony = f(x)$

Part 1. Solution of the direct problem (Using Flouqet Theorem for periodic surfaces under the assumption of Rayleigh hypotesis) 1. Solve a matrix equation [K1]*[B$_n] = [A1]forB_n2.Scatteredfieldissum(B_n * exp(i * betax_n * x + i * q_n * y))(summationfrom - NctoNc)$

q=ak0*cos(phi$_0); betax = ak0 * sin(phi_0);$

for n1=1:2*Nc+1 betax$_n(n1) = betax + 2 * (n1 - Nc1) * pi/P; end$

for nb=1:2*Nc+1, if abs(betax$_n(nb)) > ak0q_n(nb) = i*sqrt(betax_n(nb)*betax_n(nb) - ak0 * ak0); elseq_n(nb) = sqrt(ak0 * ak0 - betax_n(nb) * betax_n(nb)); endend$

for m2=1:2*Nc+1, for n2=1:2*Nc+1, K1(m2,n2)=-quad(@int2,-P/2,P/2,tolerans,0,ak0,P,q,q$_n($ $quad(@int1, -P/2, P/2, tolerans, 0, ak0, P, q, m2, Nc1, p1, p2); end$

B1=inv(K1)*A1.';

x2=p1; x10=P/2; Nx=120; delx=2*x10/Nx;

for ns=1:2*Nc+1, for nx=1:Nx+1 x1(nx)=-x10+delx*(nx-1); EN(ns)=q$_n(ns) * abs(B1(ns))^2;$

u$_{sg}er(ns, nx) = B1(ns)*exp(i*q_n(ns)*x2+i*betax_n(ns)*x1(nx)); u_{sd}1_ger(ns, nx) = i*q_n(ns)*B1(ns)*exp(i*q_n(ns)*x2+i*betax_n(ns)*x1(nx)); u_{sd}2_ger(ns, nx) = q_n(ns) * q_n(ns) * B1(ns) * exp(i * q_n(ns) * x2 + i * betax_n(ns) * x1(nx));$

u$_{ig}er(nx) = exp(i*betax*(x1(nx)) - i*q*x2); u_id1_ger(nx) = -i*q*exp(i*betax*(x1(nx)) - i * q * x2); u_id2_ger(nx) = -q * q * exp(i * betax * (x1(nx)) - i * q * x2);$

t1=rand(101); t2=t1(10,:);

fsurr(nx)=surface1(x1(nx),P,p1,p2); end end

oran=2*pi*max(fsurr)/P Etot=sum(EN);

u$_{s}ca_{g}er = sum(u_{sg}er); u_{s}ca_{d}1_{g}er = sum(u_{sd}1_{g}er); u_{s}ca_{d}2_{g}er = sum(u_{sd}2_{g}er);$

utot$_{g}er = u_{ig}er+u_{s}ca_{g}er; utot_{d}1_{g}er = u_{i}d1_{g}er+u_{s}ca_{d}1_{g}er; utot_{d}2_{g}er = u_{i}d2_{g}er+ u_{s}ca_{d}2_{g}er;$

fr1st$_{g}er = x2-utot_{g}er./utot_{d}1_{g}er; fr2nd1_{g}er = x2+(-utot_{d}1_{g}er+sqrt(utot_{d}1_{g}er.* utot_{d}1_{g}er-2.*utot_{g}er.*utot_{d}2_{g}er))./(utot_{d}2_{g}er); fr2nd2_{g}er = x2+(-utot_{d}1_{g}er- sqrt(utot_{d}1_{g}er.*utot_{d}1_{g}er-2.*utot_{g}er.*utot_{d}2_{g}er))./(utot_{d}2_{g}er);$

x2meas=max(fsurr)+5.*lambda$_0$;

x100=6*P/2; /scattered field is assumed to be measured on the line y=x2meas at Nxx1 discrete points in the interval x1 $\in (-x100, x100)$

Nxx1=570

delxx=2*x100/Nxx1;

for ns=1:2*Nc+1, for nx=1:Nxx1+1 xx1(nx)=-x100+delxx*(nx-1);

u$_{sm}eas1(ns,nx) = B1(ns)*exp(i*q_{n}(ns)*x2meas+i*betax_{n}(ns)*xx1(nx)); u_{sd}1(ns,nx) = i*q_{n}(ns)*B1(ns)*exp(i*q_{n}(ns)*x2meas+i*betax_{n}(ns)*xx1(nx)); u_{sd}2(ns,nx) = -q_{n}(ns)*q_{n}(ns)*B1(ns)*exp(i*q_{n}(ns)*x2meas+i*betax_{n}(ns)*xx1(nx));$

end end

u$_{sm}eas = sum(u_{sm}eas1);$

nois1=rand(Nxx1+1); nois2=nois1(:,19); nois21=nois1(:,37); v1=nois2.*nois2; v2=nois21.*nois21; rr=v1.*v1+v2.*v2; v3=sqrt(-2*(log(rr))./rr); noisratio=0.0; nreal=1.; nimag=2.; nabs=sqrt(nreal*nreal+nimag*nimag); nois3=noisratio*max(abs(u$_{sm}eas)$

for nji=1:Nxx1+1,

noisy(nji)=u$_{sm}eas(nji)+noisratio*(u_{sm}eas(nji))*((nreal+i*nimag)/(nabs))* nois2(nji); end$

u$_{sm}eas_{n}oisy = noisy.';$

Part 2. calculation of Fourier transform and solution of the spectral coefficient A(nu)

nu0=ak0-0.1; Nnu=140 delnu=2*nu0/Nnu; for nnx=1:Nxx1+1, for nnu1=1:Nnu+1, nu(nnu1)=-nu0+delnu*(nnu1-1);

if abs(nu(nnu1)) ¡= abs(ak0) gamma0(nnu1)=-i*sqrt(-nu(nnu1)*nu(nnu1)+ak0*ak0); else gamma0(nnu1)=sqrt(nu(nnu1)*nu(nnu1)-ak0*ak0); end

gg$_{p}ec(nnx,nnu1) = u_{sm}eas_{n}oisy(nnx)*exp(-i*nu(nnu1)*xx1(nnx))*delxx;$

end end

yy1=sum(gg$_{p}ec$);

for kk=1:Nnu+1, Anu(kk)=exp(gamma0(kk)*(x2meas))*yy1(kk); end

xx10=P/2.; Nxx=120; delx1=2*xx10/Nxx;

alphax=max(fsurr)+0.1*lambda$_0$;

for nxx=1:Nxx+1,

y2(nxx)=0.*max(fsurr)/2+0.00*lambda$_0$;$y2_dx1_01(nxx) = 0.*max(fsurr)/2 + 0.00*lambda_0; y2_dx1_02(nxx) = 0.*max(fsurr)/2 + 0.00*lambda_0;$

end

Mc=13;

for itn2=1:6, itn2

for nnu2=1:Nnu+1; for nxx=1:Nxx+1, for mm1=1:Mc, xx11(nxx)=-xx10+delx1*(nxx-1);

ui(nxx)=exp(-i*q*y2(nxx)+i*betax*xx11(nxx)); ui$_dx2_01(nxx) = (-i*q)*exp(-i*q*y2(nxx)+i*betax*xx11(nxx)); ui_dx2_02(nxx) = (-i*q)*(-i*q)*exp(-i*q*y2(nxx)+i*betax*xx11(nxx)); ui_dx1_01(nxx) = (-i*q*y2_dx1_01(nxx)+i*betax)*exp(-i*q*y2(nxx)+i*betax*xx11(nxx)); ui_dx1_02(nxx) = (-i*q*y2_dx1_02(nxx))*exp(-i*q*y2(nxx)+i*betax*xx11(nxx))...+(-i*q*y2_dx1_01(nxx)+i*betax)^2*exp(-i*q*y2(nxx)+i*betax*xx11(nxx)); ui_dx1x2_0101(nxx) = (-i*q)*(-i*q*y2_dx1_01(nxx)+i*betax)*exp(-i*q*y2(nxx)+i*betax*xx11(nxx));$

us(nnu2,nxx,mm1)=(1/prod(1:mm1-1))*((y2(nxx)-alphax)$^(mm1-1))...*(1/(2*pi))*((-1)^(mm1-1))*(gamma0(nnu2)^(mm1-1))...*Anu(nnu2)*exp(-gamma0(nnu2)*(alphax))*exp(i*nu(nnu2)*xx11(nxx))*delnu;$

us$_dx2_01(nnu2,nxx,mm1) = (mm1-1)*(1/prod(1:mm1-1))*((y2(nxx)-alphax)^(mm1-2))...*(1/(2*pi))*((-1)^(mm1-1))*(gamma0(nnu2)^(mm1-1))...*Anu(nnu2)*exp(-gamma0(nnu2)*(alphax))*exp(i*nu(nnu2)*xx11(nxx))*delnu;$

us$_dx2_02(nnu2,nxx,mm1) = ((mm1-1)*(mm1-2))*(1/prod(1:mm1-1))*((y2(nxx)-alphax)^(mm1-3))*(1/(2*pi))*((-1)^(mm1-1))*(gamma0(nnu2)^(mm1-1))...*Anu(nnu2)*exp(-gamma0(nnu2)*(alphax))*exp(i*nu(nnu2)*xx11(nxx))*delnu;$

us$_dx1_01(nnu2,nxx,mm1) = (i*nu(nnu2))*(1/prod(1:mm1-1))...*((y2(nxx)-alphax)^(mm1-1))...*(1/(2*pi))*((-1)^(mm1-1))*(gamma0(nnu2)^(mm1-1))...*Anu(nnu2)*exp(gamma0(nnu2)*(alphax))*exp(i*nu(nnu2)*xx11(nxx))*delnu...+((mm1-1)*y2_dx1_01(nxx))*(1/prod(1:mm1-1))*((y2(nxx)-alphax)^(mm12))...*(1/(2*pi))*((-1)^(mm1-1))*(gamma0(nnu2)^(mm1-1))...*Anu(nnu2)*exp(-gamma0(nnu2)*(alphax))*exp(i*nu(nnu2)*xx11(nxx))*delnu;$

us$_dx1_02(nnu2,nxx,mm1) = (i*nu(nnu2))*us_dx1_01(nnu2,nxx,mm1)...+(i*nu(nnu2))*((mm1-1)*y2_dx1_02(nxx))*(1/prod(1:mm1-1))*((y2(nxx)-alphax)^(mm1-2))...*(1/(2*pi))*((-1)^(mm1-1))*(gamma0(nnu2)^(mm1-1))...*Anu(nnu2)*exp(gamma0(nnu2)*(alphax))*exp(i*nu(nnu2)*xx11(nxx))*delnu...+(mm1-2)*y2_dx1_01(nxx)*(mm1-1)*y2_dx1_01(nxx)*(1/prod(1:mm1-1))...*((y2(nxx)-alphax)^(mm1-3))*(1/(2*pi))*((-1)^(mm1-1))*(gamma0(nnu2)(mm1-1))...*Anu(nnu2)*exp(gamma0(nnu2)*(alphax))*exp(i*nu(nnu2)*xx11(nxx))*delnu...+(mm1-1)*y2_dx1_02(nxx)*(1/prod(1:$

$mm1-1))*((y2(nxx)-alphax)^(mm1-2))*(1/(2*pi))*((-1)^(mm1-1))*(gamma0(nnu2)^(mm1-1))...*Anu(nnu2)*exp(-gamma0(nnu2)*(alphax))*exp(i*nu(nnu2)*xx11(nxx))*delnu;$

us$_dx1x2_0101(nnu2,nxx,mm1) = (i*nu(nnu2)*(mm1-1)*y2_dx1_01(nxx))*(1/prod(1:mm1-1))*((y2(nxx)-alphax)^(mm1-2))*(1/(2*pi))*((-1)^(mm1-1))*(gamma0(nnu2)^(mm1-1))...*Anu(nnu2)*exp(gamma0(nnu2)*(alphax))*exp(i*nu(nnu2)*xx11(nxx))*delnu...+(mm1-1)*y2_dx1_01(nxx)*(mm1-2)*y2_dx1_01(nxx)*(1/prod(1:mm1-1))*...((y2(nxx)-alphax)^(mm1-3))*(1/(2*pi))*((-1)^(mm1-1))*(gamma0(nnu2)^(mm1-1))*Anu(nnu2)*exp(-gamma0(nnu2)*(alphax))*exp(i*nu(nnu2)*xx11(nxx))*delnu;$

end end end

u=ui+sum(sum(us,3)); u$_dx1_01 = ui_dx1_01 + sum(sum(us_dx1_01,3)); u_dx2_01 = ui_dx2_01+sum(sum(us_dx2_01,3)); u_dx1_02 = ui_dx1_02+sum(sum(us_dx1_02,3)); u_dx2_02 = ui_dx2_02+sum(sum(us_dx2_02,3)); u_dx1x2_0101 = ui_dx1x2_0101+sum(sum(us_dx1x2_0101,3));$

for pp=1:Nxx+1,

F(pp)=(-1.*(y2$_dx1_01(pp))*u_dx1_01(pp)+u_dx2_01(pp))*(1/sqrt(1+(y2_dx1_01(pp))^2));$

F$_dx2_01(pp) = (-u_dx1_02(pp)+u_dx2_02(pp))*(1/sqrt(1+(y2_dx1_01(pp))^2))...+(-1.*(y2_dx1_01(pp))*u_dx1_01(pp)+u_dx2_01(pp))*(-0.5/((1+(y2_dx1_01(pp))^2)^1.5));$

F$_dx1_01(pp) = (1/sqrt(1+(y2_dx1_01(pp))^2)*((-(y2_dx1_02(pp))*u_dx1_01(pp)+y2_dx1_01(pp))*u_dx1_02(pp))+u_dx1x2_0101(pp))...+(-1.*(y2_dx1_01(pp))*u_dx1_01(pp)+u_dx2_01(pp))*(-0.5*y2_dx1_02(pp)/((1+(y2_dx1_01(pp))^2)^1.5));$

F$_dn_01(pp) = 1/sqrt(1+(y2_dx1_01(pp))^2)*(-y2_dx1_01(pp)*F_dx1_01(pp)+F_dx2_01(pp));$

F$_ds_01(pp) = 1/sqrt(1+(y2_dx1_01(pp))^2)*(F_dx1_01(pp)+y2_dx1_01(pp)*F_dx2_01(pp));$

end

ax=F; bx=F$_dx2_01;$

M0=78; fdirek=-ax./bx; rh=-ax;

for pp=1:Nxx+1, for mm=1:2*M0+1, mat1(pp,mm)=exp(i*(mm-M0-1).*xx11(pp)).*(bx(pp)); end end

cn1=pinv(mat1)*rh.';

for ppx=1:Nxx+1, for mm=1:2*M0+1, g1(ppx,mm)=cn1(mm)*exp(i*(mm-M0-1).*xx11(ppx)); end end

y2=y2+(real(sum(g1,2))).'; x2=0; y2$_dx1_01 = diff(y2)/delx; y2_dx1_01(121) = 2*y2_dx1_01(120)-y2_dx1_01(119); y2_dx1_02 = diff(y2_dx1_01)/delx; y2_dx1_02(121) = 2*y2_dx1_02(120)-y2_dx1_02(119);$

end

frcs=y2; toc beep

figure plot(x1,real(frcs),'k') hold plot(x1,(fsurr),'') plot(x1,imag(frcs),'g')

Rough surface definitions

int2 function y1 = int1(x,ak0,P,q,m,Nc1,p1,p2) y1=exp(-i*q*(surface1(x,P,p1,p2))).*exp(-i*2*(m-Nc1)*pi*x/P).*(-i*q + i*2* (m-Nc1)*pi*(surface2(x,P,p1,p2))/P);

function y1 = int2(x,ak0,P,q,q$_n, m, n, p1, p2$)

y1=exp(i*q$_n * (surface1(x, P, p1, p2))).*exp(i*2*(n-m)*pi*x/P).*(i*q_n - i*2*(n-m)*pi*(surface2(x, P, p1, p2))/P$);

surface1

function fs=surface1(x,P,p1,p2)

if x¿=-P/2 x¡0 fs=cos(7*pi*x/P).*(exp(-abs(x/6))).*(p1*(1+x/(P/2))); else fs=p1*(exp(-abs(x/10))).*exp(-1*x/3).*cos(5*pi*x/P); end

if x¿-P/2 x¡0 fs=24*(x/P).*cos(10*pi*x/P).*(exp(-abs(1.*x))).*(p1*(1+x/(P/2))); elseif x¡P/2-1 x¿=0 fs=26*p1*(x/P).*(exp(-abs(x/2))).*exp(-1.*x).*cos(13.*pi*x/P); else fs=0.; end

if x¿=-P/2 x¡0 fs=24*(1.2*x/P).*cos(7*pi*x/P).*(exp(-1.2*abs(x))).*(p1*(1+2.*x/(P/2))); else fs=25*p1*(x/P).*(exp(-1.1*abs(x))).*exp(-x/6).*cos(5*pi*x/P); end

if x¿=-P/2 x¡-P/3 fs=exp(-x.*x/4).*(p1*(1+x/(P/2)))*x; elseif x¿=-P/3 x¡0 fs=exp(-x.*x).*(p1*exp(-1*x).*cos(5*pi*x/P)); elseif x¿=0 x¡P/3 fs=exp(-x.*x).*(p1*exp(-1*x).*cos(5.*pi*x/P)); else fs=exp(-x.*x).*(p1*exp(-1*x).*cos(5*pi*x/P)); end

if x¿=-P/2 x¡0 fs=p1*cos(2*pi*x/P); else fs=p1*cos(2*pi*x/P); end

if x¿=-P/2 x¡0 fs=(4*p1/P)*(x+P/4); elseif x¿=0 x¡P/2 fs=-(4*p1/P)*(x-P/4); elseif x¿=P/2 x¡P fs=(4*p1/P)*(x-P+P/4); elseif x¿=P x¡=3*P/2 fs=-(4*p1/P)*(x-P-P/4); elseif x¿=-P x¡-P/2 fs=-(4*p1/P)*(x+P-P/4); else fs=(4*p1/P)*(x+P+P
end if x¿=-P/2 x¡-P/6 fs=p1/6*sin(2*pi*x/(P/3)); else fs=p1/6*(5/(24/8)-x/(P/8)); rough7 if x¿=-P/2 x¡-P/6 fs=p1/6*sin(2*pi*x/(P/3)); elseif x¿=-P/6 x¡P/12 fs=0.; elseif x¿=P/12 x¡P/3 fs=p2/6*(5/(24/8)-x/(P/8)); else fs=p1/6*(-3+x/(P/6)); end

surface2

function fs1=surface2(x,P,p1,p2)

if x¿=-P/2 x¡0 fs1=sin(7*pi*x/P).*(exp(-abs(x/6))).*(p1*(1+x/(P/2)))*(-7*pi/P)... + cos(7*pi*x/P).*(exp(-abs(x/6))).*(p1*(1+x/(P/2)))*(1/6)... + cos(7*pi*x/P).*(exp(-abs(x/6))).*(p1/(P/2)); else fs1=p1*(exp(-abs(x/10))).*exp(-1*x/3).*cos(5*pi*x/P)*(1/10)... +p1*(exp(-abs(x/10))).*exp(-1*x/3).*cos(5*pi*x/P)*(-1/3)... +p1*(exp(-abs(x/10))).*exp(-1*x/3).*sin(5*pi*x/P)*(-5*pi/P); end

if x¿-P/2 x¡0 fs1=24*(1/P).*cos(10*pi*x/P).*(exp(-abs(1.*x))).*(p1*(1+x/(P/2)))... +24*(x/P).*sin(10*pi*x/P).*(exp(-abs(1.*x))).*(p1*(1+x/(P/2)))*(-10*pi/P)... +24*(x/P).*cos(10*pi*x/P).*(exp(-abs(1.*x))).*(p1*(1+x/(P/2)))... +24*(x/P).*cos(10*pi*x,
abs(1.*x))).*(p1*(1+x/(P/2)))*(p1*2/P); elseif x¡P/2-1 x¿=0 fs1=26*p1*(1/P).*(exp(-abs(x/2))).*exp(-1.*x).*cos(13.*pi*x/P)... +26*p1*(x/P).*(exp(-abs(x/2))).*exp(-1.*x).*cos(13.*pi*x/P)*(-1/2)... +26*p1*(x/P).*(exp(-abs(x/2))).*exp(-1.*x).*cos(13.*pi*x/P
1)... +26*p1*(x/P).*(exp(-abs(x/2))).*exp(-1.*x).*sin(13.*pi*x/P)*(-13*pi/P); else fs1=0.; end

if x¿=-P/2 x¡0 fs1=24*cos(7*pi*x/P).*(exp(-1.2*abs(x))).*(p1*(1+2.*x/(P/2)))*(1.2/P)...

+24*(1.2*x/P).*sin(7*pi*x/P).*(exp(-1.2*abs(x))).*(p1*(1+2.*x/(P/2)))*(-7*pi/P)... +24*(1.2*x/P).*cos(7*pi*x/P).*(exp(-1.2*abs(x))).*(p1*(1+2.*x/(P/2)))*(1.2)... +24*(1.2*x/P).*cos(7*pi*x/P).*(exp(-1.2*abs(x))).*(4*p1/P); else fs1=25*p1*(exp(-1.1*abs(x))).*exp(-x/6).*cos(5*pi*x/P)*(1/P)... +25*p1*(x/P).*(exp(-1.1*abs(x))).*exp(-x/6).*cos(5*pi*x/P)*(-1.1)... +25*p1*(x/P).*(exp(-1.1*abs(x))).*exp(-x/6).*cos(5*pi*x/P)*(-1/6)... +25*p1*(x/P).*(exp(-1.1*abs(x))).*exp(-x/6).*cos(5*pi*x/P)*(5*pi/P); end

if x¿=-P/2 x¡-P/3 fs=exp(-x.*x/4).*(p1*(1+x/(P/2))); fs1=exp(-x.*x/4).*(p1/((P/2)))*x+(-2*x/4)*exp(-x.*x/4).*(p1*(1+x/(P/2))) x+exp(-x.*x/4).*(p1*(1+x/(P/2)));; elseif x¿=-P/3 x¡0 fs=exp(-x.*x).*(p1*exp(-1*x).*cos(5*pi*x/P)); fs1=(-2*x)*exp(-x.*x).*(p1*exp(-1*x).*cos(5*pi*x/P))+(-1)*exp(-x.*x).* (p1*exp(-1*x).*cos(5*pi*x/P))+(-5*pi/p)*exp(-x.*x).*(p1* exp(-1*x).*sin(5*pi*x/P)); elseif x¿=0 x¡P/3 fs=exp(-x.*x).*(p1*exp(-1*x).*cos(5.*pi*x/P)); fs1=(-2*x)*exp(-x.*x).*(p1*exp(-1*x).*cos(5*pi*x/P))+(-1)*exp(-x.*x).* (p1*exp(-1*x).*cos(5*pi*x/P))+(-5*pi/p)*exp(-x.*x).*(p1* exp(-1*x).*sin(5*pi*x/P)); else fs1=(-2*x)*exp(-x.*x).*(p1*exp(-1*x).*cos(5*pi*x/P))+(-1)*exp(-x.*x).* (p1*exp(-1*x).*cos(5*pi*x/P))+(-5*pi/p)*exp(-x.*x).*(p1* exp(-1*x).*sin(5*pi*x/P)); end

if x¿=-P/2 x¡0 fs1=p1*(-2.*pi/P)*sin(2*pi*x/P); else fs1=p1*(-2.*pi/P)*sin(2*pi*x/P); end

if x¿=-P/2 x¡0 fs1=(4*p1/P); elseif x¿=0 x¡P/2 fs1=-(4*p1/P); elseif x¿=P/2 x¡P fs1=(4*p1/P); elseif x¿=P x¡=3*P/2 fs1=-(4*p1/P); elseif x¿=-P x¡-P/2 fs1=-(4*p1/P); else fs1=(4*p1/P); end

if x¿=-P/2 x¡-P/6 fs1=p1/6*(2*pi/(P/3))*cos(2*pi*x/(P/3)); else fs1=p1/6*(-1/(P/8)); rough7 if x¿=-P/2 x¡-P/6 fs1=p1/6*(2*pi/(P/3))*cos(2*pi*x/(P/3)); elseif x¿=-P/6 x¡P/12 fs1=0.; elseif x¿=P/12 x¡P/3 fs1=p2/6*(-1/(P/8)); else fs1=p1/6*(1/(P/6)); end

BIOGRAPHY

Çağdaş Genç was born in Akşehir, Turkey in 1981. He received the B.S in Electronics and Telecommunication Engineering from Istanbul Technical University, Istanbul in 2003, respectively. He is currently working toward the M.S. degree at the Istanbul Technical University.